

2010-01-26

Miniature Ceramic PIFA for UWB Band Group 3 and 6

David Kearney

Technological University Dublin, david.kearney@tudublin.ie

Matthias John

Technological University Dublin, matthias.john@tudublin.ie

Max Ammann

Technological University Dublin, max.ammann@tudublin.ie

Follow this and additional works at: <https://arrow.tudublin.ie/ahfrcart>



Part of the [Systems and Communications Commons](#)

Recommended Citation

Kearney, D., John, M. & Ammann, M.J. (2010) Miniature Ceramic PIFA for UWB Band Group 3 & 6. *IEEE Antennas and Wireless Propagation Letters*, vol. 9, 2010 pp. 28-31. doi:10.1109/LAWP.2010.2041423

This Article is brought to you for free and open access by the Antenna & High Frequency Research Centre at ARROW@TU Dublin. It has been accepted for inclusion in Articles by an authorized administrator of ARROW@TU Dublin. For more information, please contact arrow.admin@tudublin.ie, aisling.coyne@tudublin.ie.



This work is licensed under a [Creative Commons Attribution-NonCommercial-Share Alike 4.0 License](#)
Funder: Science Foundation Ireland

Miniature Ceramic PIFA for UWB Band Groups 3 and 6

David Kearney, Matthias John, *Member, IEEE*, and Max J. Ammann, *Senior Member, IEEE*

Abstract—A ceramic chip planar inverted-F antenna (PIFA) is proposed for integration into a mobile handset providing UWB functionality across band groups 3 and 6. The antenna design exhibits a total efficiency of greater than 50% across the entire 6.3–9 GHz bandwidth while maintaining a very small volume of 57.6 mm³. The antenna uses a combination of the normal PIFA resonance and a second resonance due to the ceramic block to achieve a broad ultrawideband (UWB) bandwidth.

Index Terms—Ceramic chip, planar inverted-F antenna (PIFA), ultrawideband (UWB) antenna.

I. INTRODUCTION

AS THE WIRELESS communication industry expands, there is increased demand for antenna solutions that provide high performance, low cost, and small size to support the increasing number of wireless protocols. As multiple antennas are integrated into mobile handsets to provide wide-ranging functionality, size is a critical factor. For ultrawideband (UWB) devices in particular, the necessity to provide good performance over a very wide bandwidth combined with tough size restrictions presents a number of key antenna design challenges.

There is a belief by many in the industry [1], [2] that real market acceleration for UWB will only occur when UWB becomes integrated into mobile handsets, where it will be used to transfer data files at much higher data rates than those that exist with current devices. Since the volume available within a mobile handset is extremely limited, the UWB requirement for good performance over a large bandwidth poses a considerable challenge for handset antenna designers.

The FCC-approved UWB band is divided into six band groups. Compared to the bands at the lower end of the 3.1–10.6 GHz spectrum, the UWB bands above 6 GHz tend to be less restricted since there are less existing services operating at these frequencies [3]. Hence, interference is less likely than at the lower end of the UWB spectrum. There are more channels, so the potential channel capacity is greater in the higher

Manuscript received November 06, 2009; manuscript revised December 22, 2009 and January 15, 2010. Date of publication January 26, 2010; date of current version March 05, 2010. This work was supported in part by the Science Foundation Ireland.

D. Kearney is with TDK Electronics Ireland, Dublin 24, Ireland (e-mail: david.kearney78@gmail.com).

M. John and M. J. Ammann are with the Centre for Telecommunications Value-Chain Research (CTVR) and the Antenna and High Frequency Research Centre, School of Electronic and Communications Engineering, Dublin Institute of Technology, Dublin 8, Ireland (e-mail: matthias.john@dit.ie; max.ammann@dit.ie).

Color versions of one or more of the figures in this letter are available online at <http://ieeexplore.ieee.org>.

Digital Object Identifier 10.1109/LAWP.2010.2041423

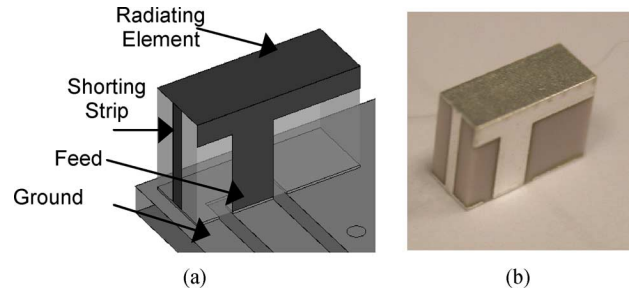


Fig. 1. Ceramic chip PIFA: (a) CST simulation model and (b) measurement prototype.

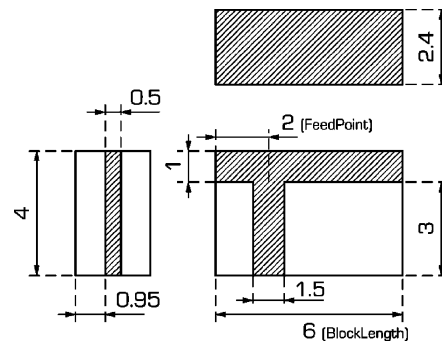


Fig. 2. Dimensions in mm of PIFA structure.

bands, with the added benefit of having smaller wavelength of operation, which requires a smaller antenna, a critical factor for mobile handset integration.

II. CERAMIC PIFA ANTENNA DESIGN

Planar inverted-F antennas (PIFAs) are popular choices for integration into mobile handsets due to their low profile, low cost, and relatively low design complexity [4]. Since the PIFA can be printed onto a ceramic block, the dielectric loading properties of the block can be harnessed to further reduce size or improve performance [5].

It is worth noting that traditionally PIFAs have mainly been used in narrowband systems [6], [7] such as Cellular, GPS, and Bluetooth, where the required bandwidth of operation of the antenna is much lower than that required for UWB.

Typical UWB antennas tend to be printed monopoles with very broad bandwidths as in [8]–[10], but these types of antennas tend to be too large for handset integration and also have the disadvantage of no ground plane running underneath, meaning a large volume around the antenna structure must be kept clear of any other components.

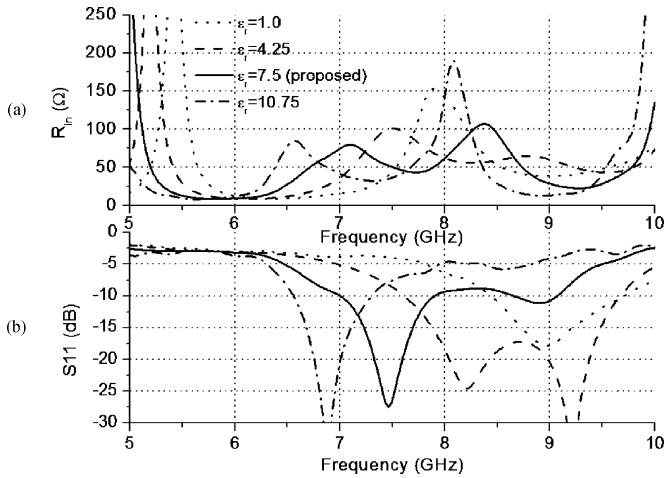


Fig. 3. (a) Real part of input impedance. (b) Return loss for different dielectric constants of the ceramic material.

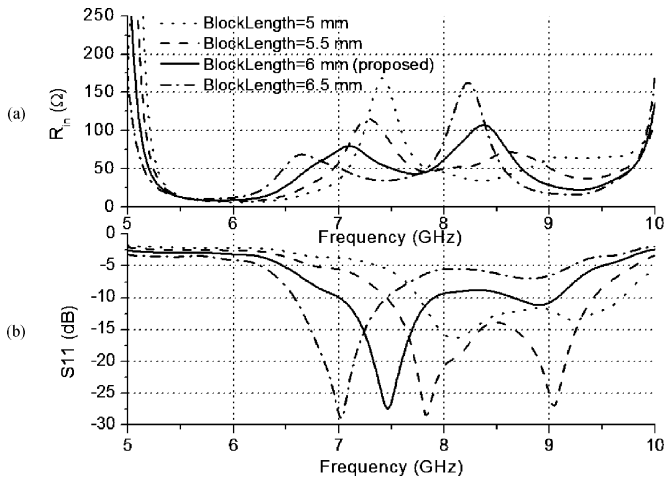


Fig. 4. (a) Real part of input impedance. (b) Return loss for different block and radiating element lengths.

A. Simulation Model

The resonant frequency of a PIFA is strongly dependant on the width W and length L of the radiating patch [6]. Extensive parameter sweeps were carried out using CST MWS with the ceramic PIFA mounted in the top left corner of a standard $80 \times 40 \text{ mm}^2$ mobile handset board. An optimized structure for the antenna was established as shown in Fig. 1. The antenna is $6 \times 4 \times 2.4 \text{ mm}^3$ in size. Fig. 2 shows detailed dimensions of the structure. A dielectric constant of $\epsilon_r = 7.5$ was chosen for the ceramic block.

B. Sweep: Dielectric Constant of Ceramic Substrate

To illustrate the key elements of the design, parameter sweeps of the dielectric constant and two critical dimensions as denoted in Fig. 2 are presented, and their effects on the performance of the antenna outlined and discussed.

Fig. 3(a) and (b) show plots of the input impedance and S_{11} of the antenna as the dielectric constant ϵ_r of the ceramic block is swept from 1.0 to 10.75. All other dimensions remain constant.

The dotted plot represents the antenna performance when $\epsilon_r = 1$. Within the 6.3–9 GHz band, a single true resonance at

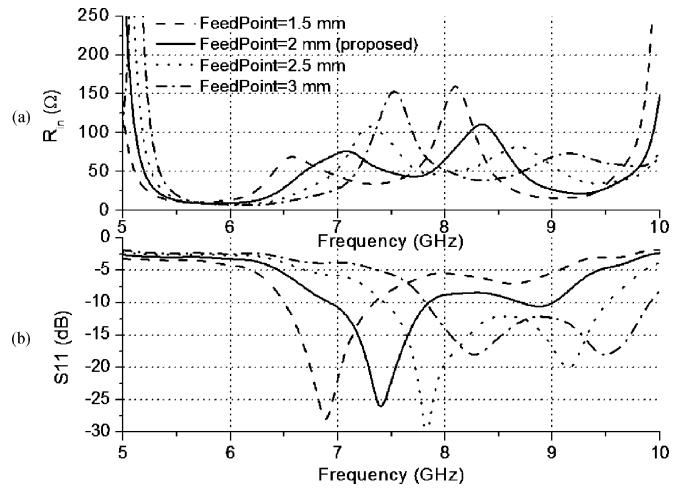


Fig. 5. (a) Real part of the input impedance. (b) Return loss for different feed-point locations.

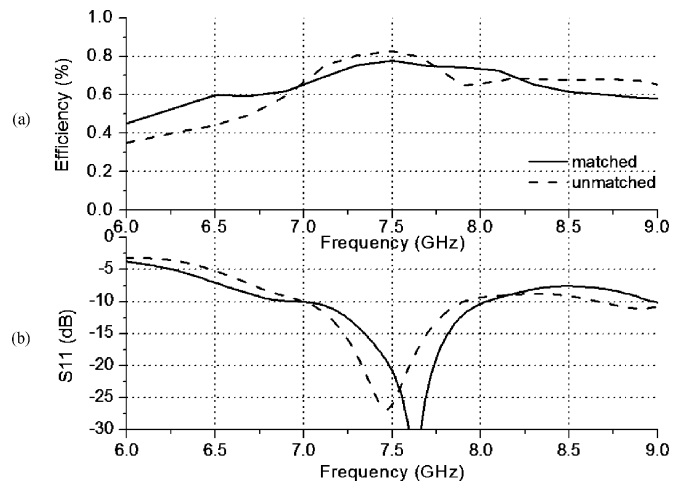


Fig. 6. Simulated matched versus unmatched (a) efficiency and (b) return loss of the UWB PIFA.

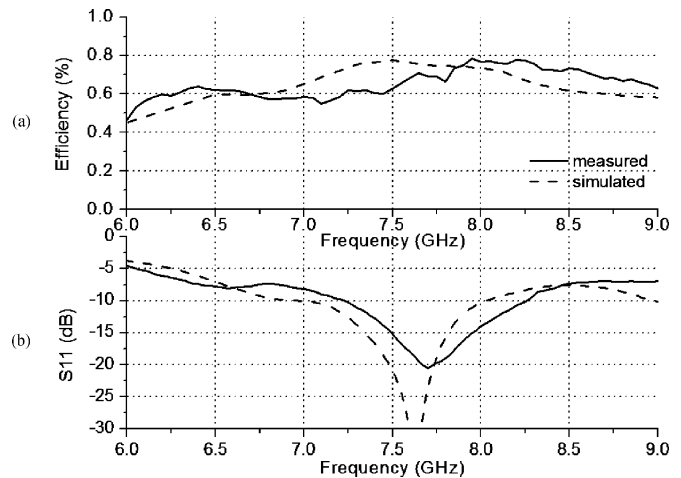


Fig. 7. Simulated versus measured (a) efficiency and (b) return loss of the UWB PIFA.

7.9 GHz can be clearly seen from the impedance plot [Fig. 3(a)], i.e., frequency at which the antenna structure is resonating corresponding to a peak in R_{in} and $jX_{in} = 0$. As ϵ_r is increased,

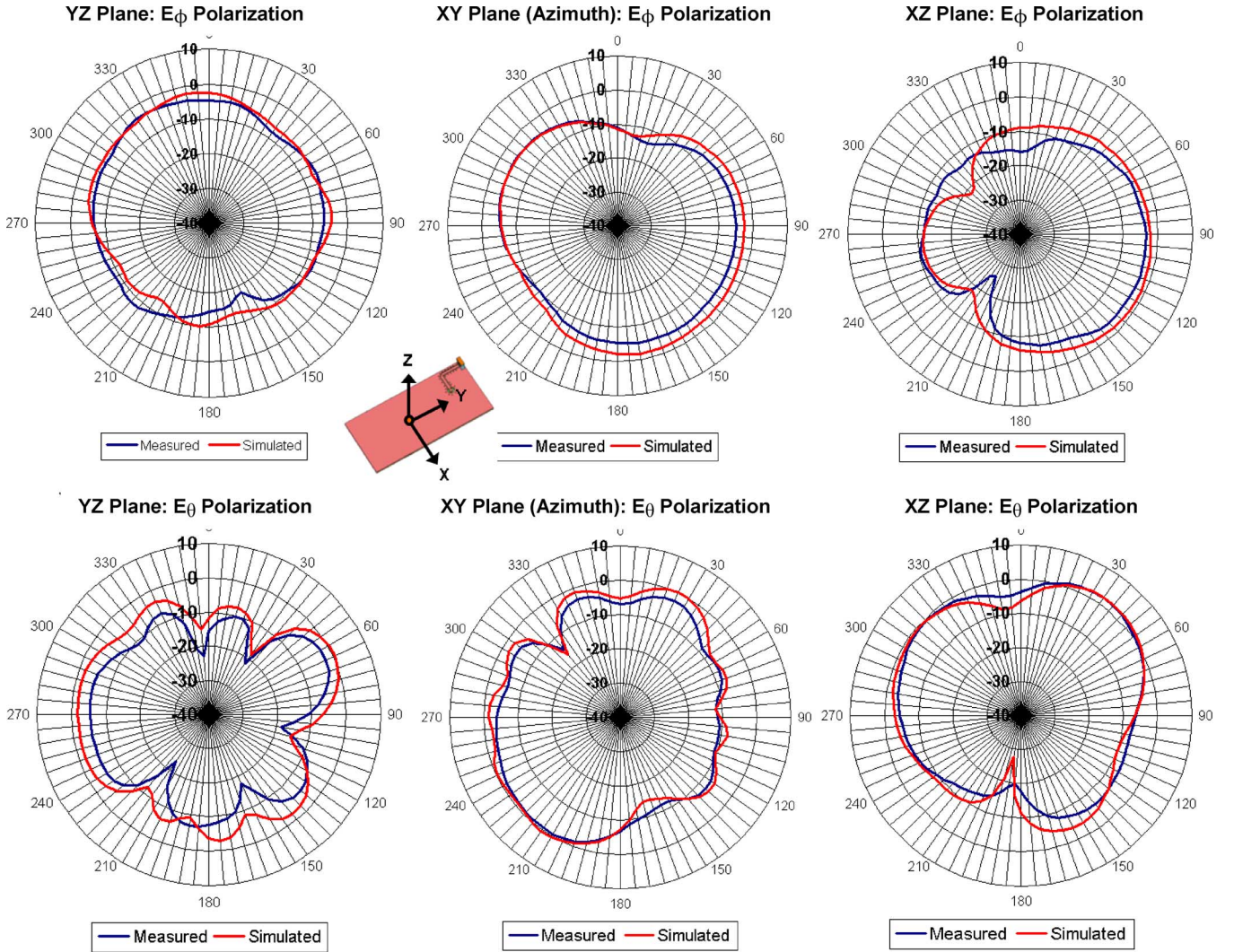


Fig. 8. Measured versus simulated radiation pattern for the UWB PIFA at 7.1 GHz.

the resonance is loaded and reduced in frequency to 7.5, 7.1, and 6.5 GHz for $\epsilon_r = 4.25$, 7.5, and 10.75, respectively. A second effect of the ceramic block is that a dielectric resonant mode is excited within the block, which resonates at a slightly higher frequency than the PIFA resonance. The single resonance that exists when $\epsilon_r = 1$ is replaced by two resonances when $\epsilon_r = 7.5$ at 7.1 and 8.4 GHz, thus providing wide bandwidth. The block resonance primarily shows sensitivity to the block length, feed-point position, and block height.

C. Sweep: Block Length and PIFA Length

Fig. 4(a) and (b) show the input impedance and S_{11} for the antenna as the length of the ceramic block and the radiating element is swept. All other dimensions of the antenna remain constant.

As can be seen from the impedance plot, both resonances are shifted down in frequency as the block and radiating element length is increased. This length directly affects the length of the current path in the PIFA, and thus the lower resonance is reduced. Similarly, the dielectric resonant length of the ceramic block is increased, and the frequency of the upper resonance is reduced.

The input impedance match at the resonant frequencies is also affected. As the block and radiating element length is increased, the value of R_{IN} decreases at the lower resonance and increases at the upper resonance. For the proposed antenna, a block length was chosen that provides the best balance between the matches at these two resonances, and thus the best overall match across the band. A block and radiating element length of around 6 mm allows for good combination of the resonances and exhibits a very broad -6 dB bandwidth of around 6.5–9.4 GHz.

D. Sweep: Feed Position

The importance of the feedpoint position is analyzed by examining a parameter sweep of the distance of the feedpoint from the edge of the dielectric block while the shorting strip remains stationary. Adjusting the feed position to give an input impedance closest to 50Ω across the band allows for optimization of the return loss, and thus the overall performance of the antenna.

Fig. 5 shows the input impedance and S_{11} versus frequency as the position of the feedpoint is swept. As the feedpoint is moved closer to the open-circuit end of the antenna, the current path, and thus the overall resonant length, decreases. The lower

resonance of the PIFA is shifted up. The upper resonance of the dielectric block is also shifted up in frequency, as the block becomes excited further from its edge.

As the feed approaches to the open-circuit end of the antenna, the E -field increases and the current decreases, increasing the input impedance. An optimal feed position was found to be 2 mm, resulting in an impedance very close to 50Ω at the lower resonance, and thus a broad -6 dB return loss bandwidth.

III. EXTERNAL MATCHING

In simulation (Fig. 6), the antenna achieves the desired performance over the majority of the 6.3–9 GHz bandwidth. However, its performance at the lower end of the band, around 6.3–6.5 GHz, does not meet the required UWB efficiency and S_{11} specifications ($S_{11} < -6$ dB and $\eta > 50\%$). An external matching circuit was implemented and optimized using capacitor and inductor components. The final optimized matching circuit consists of a capacitor of 0.75 pF in series and a shunt inductor of 0.8 nH. The effect of this matching circuit on the efficiency and S_{11} performance of the antenna is shown in Fig. 6. With matching, the return loss of the antenna is improved at the lower end of the band, and the antenna now exhibits a total efficiency of greater than 50% across the entire 6.3–9 GHz bandwidth.

IV. ANTENNA MEASUREMENT

A. S_{11} and Efficiency

Measurement prototypes of the UWB PIFA were built and analyzed to validate the simulated data. The antenna shown in Fig. 1(b) was manufactured using a standard ceramic block printing process, which prints the required antenna pattern onto the faces of a block of ceramic material using an aluminum paste. Measurements were made with the antenna mounted on a standard 80×40 mm² mobile handset test board.

Measured and simulated efficiency and S_{11} across the 6.3–9 GHz UWB bandwidth are compared in Fig. 7. The plot shows good agreement between measured and simulated data. The total efficiency across the 6.3–9 GHz band for the measured prototype is greater than 50% (and, for the most part, greater than 60%). The measured antenna also achieves the required S_{11} of better than -6 dB across the entire UWB band groups 3 and 6.

B. Radiation Pattern

Fig. 8 shows a comparison of the radiation patterns of the measured prototype versus simulated data at the resonant frequency of 7.1 GHz using the coordinate system in the inset. The radiation patterns are shown for E_θ and E_ϕ components for each cut. The plots show good agreement. Although some nulls are evident, the patterns tend to be generally omnidirectional. A maximum gain of 2.44 dBi was measured at 7.1 GHz, in reasonable agreement with the simulated prediction of 3.18 dBi.

V. CONCLUSION

A ceramic chip PIFA has been proposed to enable UWB functionality in band groups 3 and 6 in a mobile handset. The antenna uses a combination of the normal PIFA resonance and a second resonance due to the ceramic block to achieve a broad UWB bandwidth. It meets the specifications required by UWB across the 6.3–9 GHz bands while occupying a very small volume of 57.6 mm³. Critical dimensions have been examined, and the operation of the PIFA has been illustrated by analyzing return loss, input impedance, efficiency, and radiation pattern. Predicted results have been validated by measurements, which correlated well with simulated data.

REFERENCES

- [1] D. McEuen, "The UWB market shakeout," ABI Research, Nov. 2008.
- [2] B. O'Rourke, "UWB 2008: Short-term problems and long-term potential," InStat Research, Dec. 2008.
- [3] J. Lansford, "UWB in the 6 to 10-GHz spectrum present opportunities and challenges," 2008 [Online]. Available: <http://electronicdesign.com/Articles/Index.cfm?AD=1&ArticleID=19691>
- [4] Z. N. Chen and M. Y. W. Chia, *Broadband Planar Antennas*. Hoboken, NJ: Wiley, 2006.
- [5] M.-R. Hsu and K.-L. Wong, "Ceramic chip antenna for WWAN operation," in *Proc. Asia-Pacific Microw. Conf.*, 2008, pp. 1–4.
- [6] D. M. Nashaat and H. A. Elsadek, "Single feed compact quad-band PIFA antenna for wireless communication applications," *IEEE Trans. Antennas Propag.*, vol. 53, no. 8, pp. 2631–2635, Aug. 2005.
- [7] Z. Li, Y. Rahmat-Samii, and T. Kaiponen, "Bandwidth study of a dual band PIFA on a fixed substrate for wireless communication," in *Proc. IEEE Antennas Propag. Soc. Int. Symp.*, 2003, vol. 1, pp. 435–438.
- [8] D. Tsamakidis and Z. Wu, "Modeling and experimental study of dielectric loaded monopoles for UWB applications," in *Proc. IEEE Antennas Propag. Soc. Int. Symp.*, 2007, pp. 541–544.
- [9] Z. N. Chen, T. S. P. See, and X. Qing, "Small printed ultra-wide-band antenna with reduced ground plane effect," *IEEE Trans. Antennas Propag.*, vol. 55, no. 2, pp. 383–388, Feb. 2007.
- [10] M. John and M. J. Ammann, "Antenna optimization with a computationally efficient multi-objective evolutionary algorithm," *IEEE Trans. Antennas Propag.*, vol. 57, no. 1, pp. 260–263, Jan. 2009.